



## EARTHQUAKE ECONOMIC LOSSES IN MOMENT-RESISTING STEEL FRAMES EQUIPPED WITH FLUID VISCOUS DAMPERS

B. Chalarca <sup>(1)</sup>, A. Filiatrault <sup>(2)</sup>, D. Perrone <sup>(3)</sup>

<sup>(1)</sup> Ph.D. Candidate, University School for Advanced Studies IUSS Pavia, Italy, [bryan.chalarca@iusspavia.it](mailto:bryan.chalarca@iusspavia.it)

<sup>(2)</sup> Professor, University School for Advanced Studies IUSS Pavia, Italy & Department of Civil, Structural and Environmental Engineering, State University of New York at Buffalo, USA [andre.filiatrault@iusspavia.it](mailto:andre.filiatrault@iusspavia.it)

<sup>(3)</sup> Postdoctoral Researcher, University School for Advanced Studies IUSS Pavia, Italy, [daniele.perrone@iusspavia.it](mailto:daniele.perrone@iusspavia.it)

### **Abstract**

The implementation of fluid viscous dampers can improve the seismic performance of a structure, especially in terms of collapse capacity and inter-story drift reduction. However, little attention has been given to the acceleration demand on non-structural elements attached to viscously damped structures and how the different parameters (*i.e.* velocity exponent, level of added supplemental damping, damping constant distribution and brace stiffness) involved in the design of viscous dampers affect the acceleration demand. Recent earthquakes worldwide have demonstrated the great impact of acceleration-sensitive non-structural elements on the total economic losses, as these elements represent a large part of the total building investment. In order to assess the impact of implementing fluid viscous dampers on the expected annual losses of buildings, three steel moment-resisting frame archetypes of different heights and dynamic properties were equipped with linear and nonlinear viscous dampers incorporating six different velocity exponents, designed by two different approaches for three targeted added supplemental damping ratios (total of 111 archetype buildings). Incremental dynamic analyses were carried out with the FEMA P-695 far-field ground motion set scaled to ten different intensities. The collapse fragility functions, the median peak inter-story drifts, the median peak floor accelerations, and the median residual drifts were then calculated. Based on these results and furnishing the buildings with typical non-structural elements for office use, the FEMA P-58 loss estimation methodology was applied to estimate the expected annual losses for all building archetypes. The numerical results show that the different parameters involved in the design of fluid viscous dampers have an important impact on the acceleration demand of non-structural elements, and thereby, in the expected annual losses of the archetype buildings.

*Keywords: Expected Annual Losses; Fluid Viscous Dampers; Steel Moment-Resisting Frames; Acceleration-Sensitive Non-structural Elements.*



## 1. Introduction

During the last decades, several methodologies and technologies (i.e. fluid viscous dampers, rocking systems, seismic isolation, etc.) have been developed to improve the seismic performance of structures by controlling the inter-story drifts and reducing the formation of plastic hinges in the structural members [1]. However, little attention has been paid to the effects of the implementation of such devices on the seismic acceleration demand on the non-structural elements. The significant economic losses caused by the damage on acceleration-sensitive non-structural elements during recent strong earthquakes support the importance of using the acceleration demand to assess the seismic performance of a building.

Adding supplemental damping through fluid viscous dampers has been demonstrated to be a feasible technic to improve the structural behavior of existing buildings [1- 4]. However, the parameters involved in the design of the dampers (i.e. velocity exponent, targeted supplemental damping, damper's distribution, and brace stiffness), modify the seismic response of the structure, affecting significantly the acceleration demand on the non-structural elements [5]. The mathematical model that represents the force-velocity relationship in a fluid viscous damper is given by [1]:

$$F(t) = C \operatorname{sgn}(\dot{x}(t)) * |\dot{x}(t)|^\alpha \quad (1)$$

where  $F(t)$  is the force in the damper,  $C$  is the damping constant,  $\operatorname{sgn}$  is the sign function,  $\dot{x}(t)$  is the relative velocity between the two ends of the damper at time  $t$ , and  $\alpha$  is the velocity exponent that rules the hysteretic behavior of the viscous damper (Fig. 1). If  $\alpha$  is equal to unity, there is a linear relationship between the force and the velocity. When  $\alpha$  is smaller than unity, the device exhibits a nonlinear relationship between the force and the velocity limiting the maximum force at high device's velocities. The velocity exponent also modifies the hysteresis loop shape of the viscous damper. In the case of linear dampers, the hysteresis loop shows an elliptical shape, for which the maximum forces in the damper are out of phase with respect to the maximum displacements of the structure. As the velocity exponent is reduced, the hysteresis loop becomes flatter with a more rectangular shape, resembling that of a hysteretic damper and, thereby, inducing larger forces in a wider range of displacements. (Fig. 1).

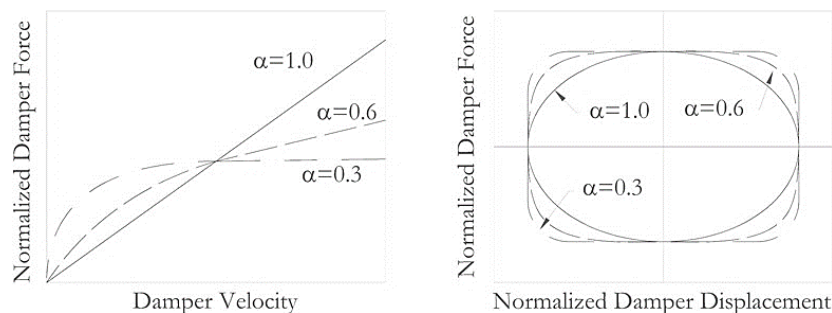


Fig. 1 - Force – velocity and force-displacement hysteresis response for viscous dampers with different velocity exponent [after 1].

In this study, the effects of implementing fluid viscous dampers on the earthquake economic losses in steel buildings were investigated. Three moment-resisting frames assumed to be located in Los Angeles, USA, were selected from the SAC Steel Project [6] as archetype buildings. The archetype buildings were retrofitted with fluid viscous dampers following two different design approaches: 1) a uniform distribution design approach (UD) in which a unique damping constant is assigned to all the dampers, and 2) an equivalent lateral stiffness design approach (ELS) in which the damping constants are distributed based on the lateral floor stiffness, thereby preserving approximately proportional damping. The fluid viscous dampers were designed to provide supplemental damping of 10%, 20%, and 35% of critical in the first elastic mode of vibration of each archetype building. An incremental dynamic analysis was carried out using the FEMA P-695 far-field (44 records) ground motions set [7] scaled to 10 different intensities. The collapse fragility functions, median peak inter-story and residual drifts, median peak floor absolute accelerations and median floor absolute acceleration



response spectra were computed from the results. Finally, the PEER-PBEE framework embodied in the FEMA P-58 methodology [8] was used to calculate the earthquake expected economic annual losses expected in the archetype buildings when supplied with typical non-structural elements for office use.

## 2. Archetype Buildings and Computational Modeling

Three moment-resisting steel frame buildings of three, six and nine stories were selected as archetype buildings for this study. The buildings were selected from the SAC Steel Project in California [6] and assumed to be located in Los Angeles (USA). The three-story archetype building was adapted from the FEMA 440 document [9]. The North-South frame was selected for this study (Fig. 2). The fundamental period is equal to 0.72 s.

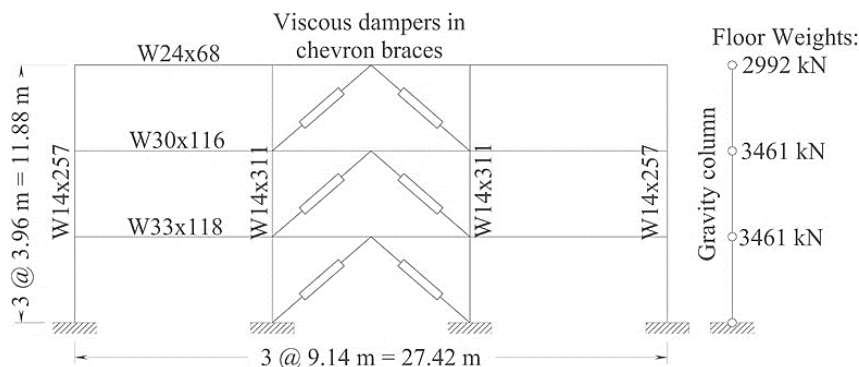


Fig. 2 - Three-story archetype building.

The six-story archetype building was initially proposed by Tsai and Popov [10] and modified by Hall [11]. The North-South frame was selected for this study (Fig. 3). This frame is characterized by a fundamental period equal to 1.3 s. Finally, the nine-story archetype building was adapted from the FEMA 440 document [9]. The selected frame for this study is shown in Fig. 4. The fundamental period is equal to 1.72 s. For all the archetype buildings, the seismic force-resisting system is composed of moment-resisting frames along the building's perimeter; the interior columns are assumed to carry only gravity loads. The beam-column connections exhibit a brittle failure mechanism typical of frames designed before the 1994 Northridge earthquake. The following assumptions and properties were considered for modeling each archetype building [1]:

- Only one exterior frame was modeled with a gravity (leaning) column that represents the interior gravity columns. Due to the building's symmetry, only half of the building was modeled. The columns were fixed at the ground level except for the gravity column that was assumed pinned at each level.
- Rigid diaphragms were simulated by constrained horizontally the nodes at the same height. The slab participation as a composite beam was not included.
- A lumped plasticity approach was assumed to simulate plastic hinges at the end of the structural members. Due to software limitations, the moment-axial force interaction was not considered. The plastic hinges had a length equal to 90% of the element depth and were characterized by a bilinear hysteretic behavior with 2% of curvature strain hardening. The expected yield strength was set equal to 290 MPa. A strength degradation model was added to account for the brittle beam-column joint failure mechanism.
- The panel zones of the beam-column connections were assumed stiff and strong enough to avoid any shear deformation and yielding. All the hysteretic energy must be dissipated through the formation of plastic hinges at the end of the members. Rigid-end offsets were set at the end of the elements to account for the size of the elements at the joints.
- Each model was characterized by an initial stiffness proportional Rayleigh damping with 5% of critical damping applied to the first and the second elastic modes of vibration.



- The viscous dampers were attached to chevron braces in the central bay of each moment-resisting frame. The dead loads induced by the chevron frames and the dampers were ignored.

The numerical models were constructed using the OpenSees software [12] in which the beams and columns were modeled with “BeamWithHinges” elements. The fluid viscous dampers were modeled with the “ViscousDamper” material that represents a Maxwell fluid that is composed of a dashpot and a spring in series. The “ViscousDamper” material was assigned to “TwoNodeLink” elements and the Maxwell fluid’s stiffness was set as 150 kN/mm.

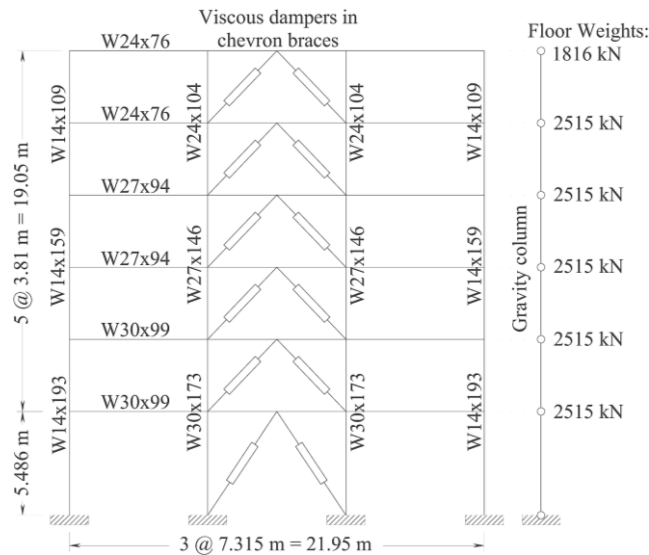


Fig. 3 - Six-story archetype building.

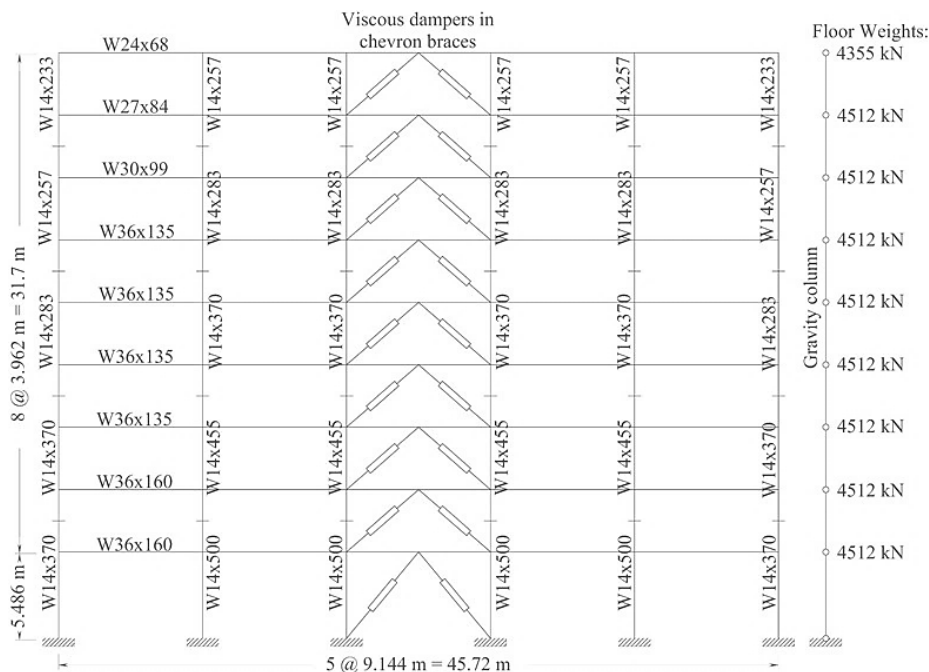


Fig. 4 - Nine-story archetype building.

### 3. Design of Fluid Viscous Dampers

The fluid viscous dampers were designed following two different distributions of damping constants: 1) a uniform distribution (UD) in which a unique damping constant was assigned to all the dampers, and 2) an



equivalent lateral stiffness (ELS) design approach in which the damping constants were distributed based on the floor stiffness, thereby approximately maintaining proportional damping. A complete explanation of both damper design approaches can be found in Christopoulos and Filiatrault [1].

### 3.1 Uniform damping distribution design approach (UD)

According to this design approach, a unique damping constant is given to all viscous dampers installed in the building. The procedure proposed by Zhang and Soong [13] and Lopez-Garcia [14] was used to calculate the single damping constant,  $C$ , along the building's height and is defined by the following equation:

$$C = \frac{\xi_1 T_1^\alpha \sqrt{\pi} \sum_{i=1}^{N_f} k_i \delta_i^2}{(2\pi)^\alpha \left( \frac{\Gamma\left(1 + \frac{\alpha}{2}\right)}{\Gamma\left(\frac{3}{2} + \frac{\alpha}{2}\right)} \right) \sum_{i=1}^{N_d} \delta_i^{\alpha+1} \cos^{\alpha+1}(\gamma_i)} \quad (2)$$

where  $\xi_1$  is the targeted supplemental first modal damping ratio,  $T_1$  is the fundamental period of the structure,  $N_f$  is the number of stories,  $k_i$  is the stiffness of the story  $i$ ,  $\delta_i$  is the inter-story drift that was calculated from the inelastic mode shape [15],  $\Gamma$  is the gamma function,  $N_d$  is the total number of dampers in the frame, and  $\gamma_i$  is the inclination angle of the  $i^{\text{th}}$  damper. The resulting damping constants calculated following the UD design approach are shown in Table 1.

Table 1 - Uniform Distribution damping constants for the three archetype buildings.

$\xi_1$	Frame	$C$ (kN s $^\alpha$ /mm $^\alpha$ )					
		$\alpha = 1.0$	$\alpha = 0.9$	$\alpha = 0.7$	$\alpha = 0.5$	$\alpha = 0.3$	$\alpha = 0.2$
10%	3-story	2	5	17	64	238	457
	6-story	5	9	29	90	274	475
	9-story	13	23	72	225	698	1221
20%	3-story	5	9	35	129	477	914
	6-story	10	19	58	179	548	951
	9-story	25	45	144	451	1396	2442
35%	3-story	8	16	61	226	834	1600
	6-story	18	32	101	314	958	1664
	9-story	45	79	252	789	2443	4274

### 3.2 Equivalent lateral stiffness design approach (ELS)

This approach distributes the damping constant along the building's height based on the floor lateral stiffness. The damping constant at a story  $n$  can be calculated from the floor lateral stiffness since the implementation of linear viscous dampers in regular structures produces approximately a stiffness proportional damping matrix [1]. In order to calculate linear viscous damping constants, elastic springs with stiffness,  $\hat{k}_0$ , are first located at the exact position of the dampers. The stiffness of the spring should be set by keeping the original floor stiffness ratios. The period of the braced structure,  $\hat{T}_1$ , should be equal to [1]:

$$\hat{T}_1 = \frac{T_1}{\sqrt{2\xi_1 + 1}} \quad (3)$$

where  $T_1$  is the fundamental period of the original (unbraced) structure and  $\xi_1$  is the target first modal damping ratio. The damping constants for the linear viscous dampers,  $C_L$ , are then calculated from:

$$C_L = \frac{T_1}{2\pi} \hat{k}_0 \quad (4)$$



For the design of the nonlinear viscous dampers ( $\alpha < 1$ ), an energy-based methodology is used in which a nonlinear viscous damping constant is calculated by equating the energy dissipated in one cycle for an equivalent linear viscous damper, as expressed mathematically by the following equation:

$$C_{NL} = C_L \frac{\sqrt{\pi}}{2} (\omega X_0)^{1-\alpha} \frac{\Gamma\left(\frac{3}{2} + \frac{\alpha}{2}\right)}{\Gamma\left(1 + \frac{\alpha}{2}\right)} \quad (5)$$

where  $\omega$  is the input frequency assumed as the fundamental frequency of the frame, and  $X_0$  is the displacement amplitude taken as the median plus one standard deviation of the relative displacement of the linear viscous dampers for a given floor from the nonlinear time history analysis at maximum credible earthquake (MCE) intensity (Spectral acceleration at a period of one second  $S_a(T=1 \text{ s}) = 0.9 \text{ g}$ ). The resulting damping constants calculated following the ELS design approach are shown in Table 2. For each value of  $\alpha$ , the left column lists the  $C$  constants of the six and three-story archetype buildings, the right column lists the  $C$  constants of the nine-story archetype building.

Table 2 - Equivalent Lateral Stiffness damping constants for the three archetype buildings.

$\xi_1$	Story Level	$C$ (kN s $^\alpha$ /mm $^\alpha$ )											
		$\alpha = 1.0$		$\alpha = 0.9$		$\alpha = 0.7$		$\alpha = 0.5$		$\alpha = 0.3$		$\alpha = 0.2$	
		6 / 3 story	9 story	6 / 3 story	9 story	6 / 3 story	9 story	6 / 3 story	9 story	6 / 3 story	9 story	6 / 3 story	9 story
10%	6 9	4	4	5	6	12	15	27	37	60	89	91	139
	5 8	4	6	6	10	14	25	35	65	88	167	139	266
	4 7	5	9	7	14	19	36	50	90	130	224	211	352
	3 6	6	12	9	19	26	45	73	109	209	261	352	404
	2 5	6	10	9	16	28	44	87	120	265	320	462	523
	1 4	5	13	8	21	26	58	84	155	273	413	491	675
	3 3	1	15	2	24	6	65	19	172	63	452	116	732
	2 2	2	16	3	26	12	70	41	185	144	489	270	794
	1 1	3	15	5	25	18	69	62	189	217	516	406	851
20%	6 9	8	8	10	12	22	29	46	68	97	160	141	244
	5 8	8	12	11	19	26	48	62	122	147	305	227	481
	4 7	10	18	14	28	35	70	87	174	215	429	340	671
	3 6	11	24	16	37	43	89	116	213	311	507	510	780
	2 5	13	20	20	33	56	86	161	227	461	595	780	962
	1 4	9	26	14	42	45	111	141	292	445	764	789	1233
	3 3	3	30	5	49	15	127	48	333	151	864	269	1391
	2 2	4	32	7	52	22	136	74	357	251	929	461	1497
	1 1	6	30	10	50	32	135	109	366	363	988	663	1620
35%	6 9	15	14	19	21	38	49	75	113	150	260	213	393
	5 8	14	21	19	33	43	82	99	203	226	500	343	783
	4 7	18	32	25	50	59	125	140	308	333	756	514	1183
	3 6	20	42	28	65	70	158	177	381	444	914	703	1413
	2 5	23	35	33	57	89	149	238	389	635	1011	1039	1627
	1 4	17	46	26	74	80	195	241	508	731	1317	1272	2117
	3 3	5	53	8	86	23	225	68	587	204	1526	353	2456
	2 2	8	56	13	91	40	239	128	626	407	1631	726	2629
	1 1	11	53	17	88	55	240	173	653	545	1770	968	2909



#### 4. Ground Motions Set and Analyses

The far-field ground motions set included in the FEMA P-695 methodology [7] was used to carry out incremental dynamic analyses. The 44 records of the ground motions set were scaled to ten different intensities based on their median spectral acceleration at a period of one second (ranging from  $S_a(T=1\text{ s}) = 0.36\text{ g}$  to  $3.6\text{ g}$ ). Figure 5 shows the median acceleration response spectra of the FEMA P-695 far-field ground motions set scaled to the equivalent design intensity (DE), as well as the ASCE 7-16 [16] design response spectrum. The collapse fragility functions for the archetype buildings were calculated with the corrections proposed by the FEMA P-695 methodology [7] and applying the maximum likelihood lognormal estimation method proposed by Baker [17]. Additionally, after removing the records that caused the collapse of the archetype buildings, the median peak and residual inter-story drifts, the median peak floor absolute accelerations and the median 5% damped floor absolute acceleration spectra were calculated. Finally, the expected losses were calculated by assigning in the archetype buildings typical non-structural elements for office use and following the procedures established by the FEMA P-58 procedure [8] for an intensity type assessment.

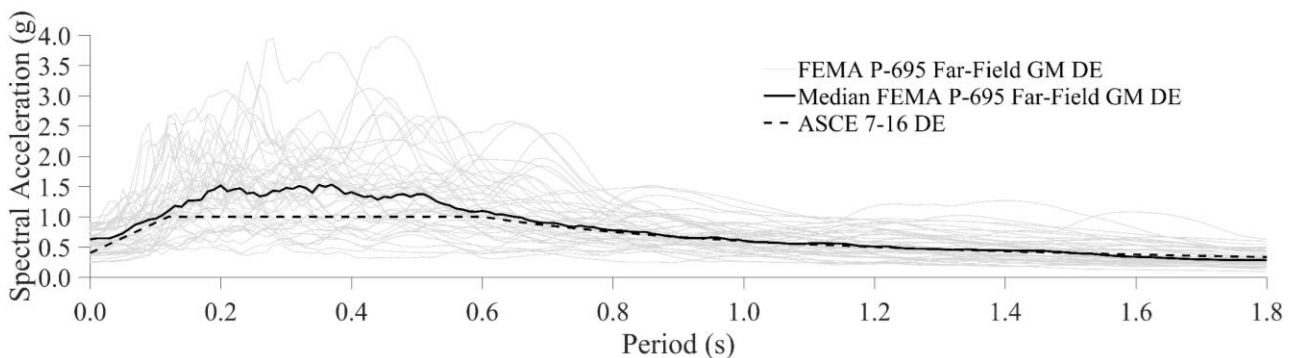


Fig. 5 - FEMA P-695 far-field ground motions (GM) set acceleration response spectra scaled to the design earthquake (DE) and the ASCE 7-16 acceleration design spectrum.

#### 5. Analysis Results

Based on the results of the incremental dynamic analyses carried out with the FEMA P-695 [7] far-field ground motions set, the collapse fragility functions, the median peak and residual inter-story drifts, the median peak floor absolute accelerations and the median 5% damped floor absolute acceleration response spectra were calculated for all the archetype buildings, i.e. the control frames (non-retrofitted) and the retrofitted frames with different fluid viscous damper configurations.

##### 5.1 Collapse fragility functions

Collapse fragility functions were calculated for the three archetype buildings following the FEMA P-695 methodology [7] and the probabilities of collapse for the DE and MCE intensities ( $S_a(T=1\text{ s}) = 0.6\text{ g}$  and  $0.9\text{ g}$ , respectively) were obtained. Due to space limitations, only the probability of collapse of the six-story building at the MCE intensity level is reported in Fig. 6. Similar results were obtained for the three and nine-story buildings. The implementation of fluid viscous dampers significantly reduces the probability of collapse. As expected, the reduction is larger as the targeted damping ratio increases. The velocity exponent and the distribution of damper constants also influence the probability of collapse. As the velocity exponent is reduced, the probability of collapse tends to increase for all the damper configurations. In general, the probability of collapse of the archetype buildings equipped with viscous dampers designed following the ELS distribution of damper constants exhibits a smaller probability of collapse than that of the UD distribution of damping constants.

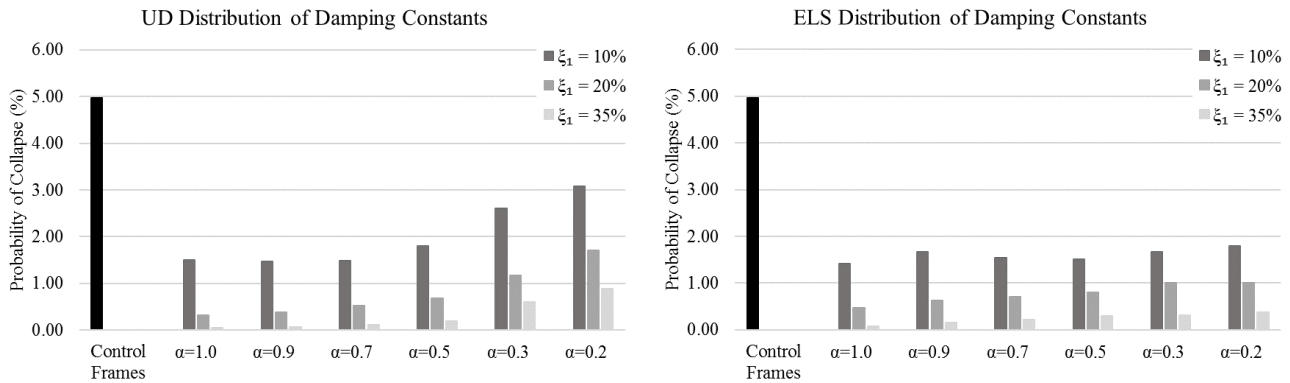


Fig. 6 - Probabilities of collapse of the six-story archetype buildings at MCE intensity level.

## 5.2 Inter-story drifts

The archetype buildings retrofitted with fluid viscous dampers experienced smaller median peak inter-story drifts than the control frames. Figure 7 shows an illustrative example of the median peak inter-story drifts for the nine-story frame with 20% supplemental damping at the DE intensity level. The three-story frame exhibited better performance when retrofitted with nonlinear viscous dampers with the lowest targeted supplemental damping (10% of critical). As the targeted damping ratio was increased, frames equipped with dampers with low values of velocity exponent experienced larger median peak inter-story drifts than the frames equipped with linear dampers or with dampers with velocity exponents close to unity. This trend was observed for both distributions of damping constants (UD and ELS). For the six and nine-story archetype frames, the buildings equipped with nonlinear viscous dampers incorporating the ELS distribution of damping constants performed better in the lower floors and performed worse at the top floor for low levels of supplemental damping (10% and 20% of critical). As the added damping is increased, the buildings equipped with dampers with low velocity exponents (i.e.  $\alpha = 0.3$  and  $0.2$ ) exhibits larger inter-story drifts along the buildings' height. This trend is even more evident for the dampers incorporating the UD distribution of damper constants.

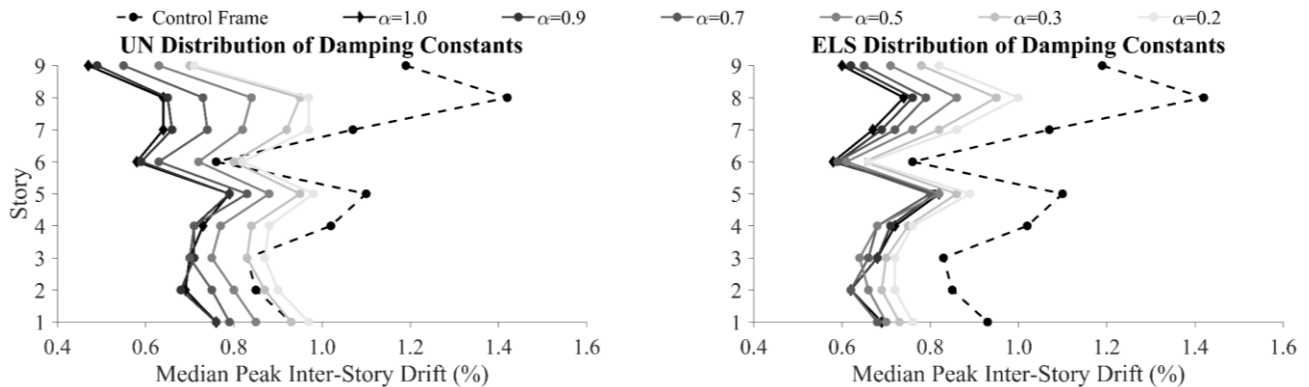


Fig. 7 - Median peak inter-story drift of the nine-story archetype building with 20% of supplemental damping at the DE intensity level.

## 5.3 Floor absolute accelerations

A reduction in the median absolute peak floor accelerations was often observed when viscous dampers were incorporated in the archetype buildings. Figure 8 shows an illustrative example of the median peak floor absolute accelerations of the three-story building assuming 35% of supplemental damping at the DE intensity level. As the targeted damping ratio is increased and the velocity exponent is reduced, the median peak floor absolute accelerations increase, reaching values larger than that of the non-retrofitted archetype buildings. This trend is evident for the frames equipped with dampers designed with 35% damping and low velocity exponents (i.e.  $\alpha = 0.3$  and  $0.2$ ). Additionally, the frames equipped with dampers incorporating the UD distribution of



damping constants performed worse compared to that of dampers incorporating the ELS distribution of damper constants.

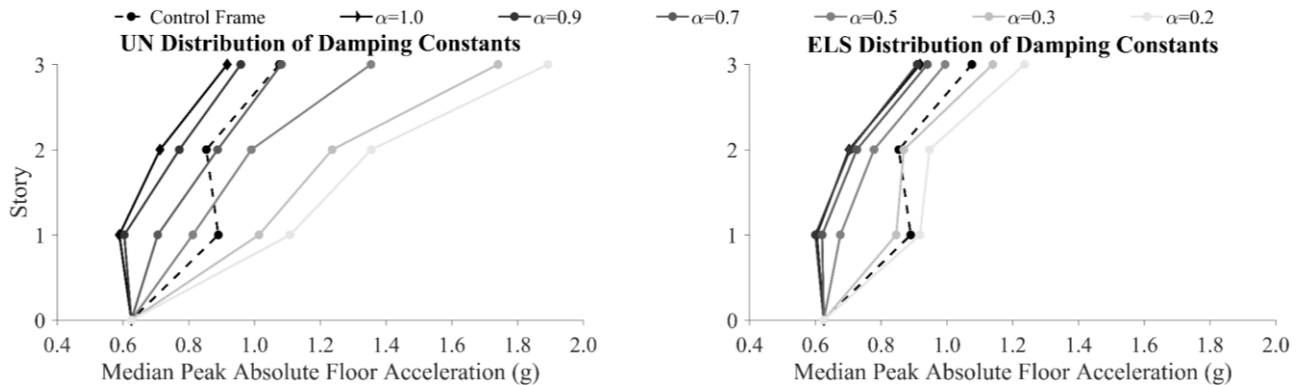


Fig. 8 - Median peak floor absolute acceleration of the three-story archetype building with 35% of supplemental damping at the DE intensity level.

A similar trend was observed in terms of floor absolute acceleration spectra. Figure 9 shows an illustrative example of the median floor absolute acceleration spectra for the three-story building with 35% of supplemental damping at the DE intensity level. The buildings equipped with dampers with low values of velocity exponent and high targeted damping ratios exhibit larger maximum spectral accelerations compared to that of the non-retrofitted buildings, having amplifications up to four times the values of the control frames.

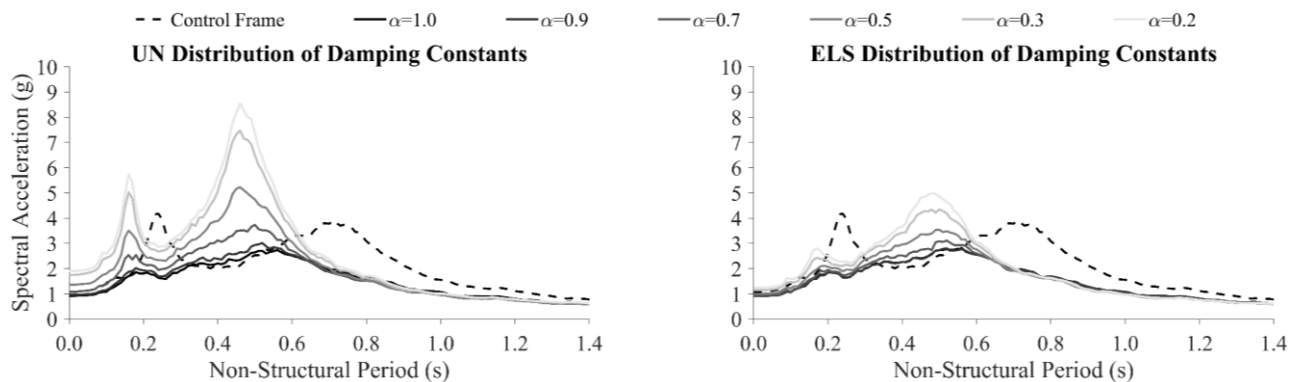


Fig. 9 - Median floor absolute acceleration spectra of the top floor of the three-story archetype building with 35% of supplemental damping at the DE intensity level.

#### 5.4 Expected annual losses

The expected annual losses were estimated following the FEMA P-58 methodology [8], assuming an intensity assessment type. The hazard curve was taken for Los Angeles, California. A total of 1000 realizations were used for the three and six-story archetype buildings and 500 realizations for the nine-story archetype building. The non-structural elements were defined assuming that the archetype buildings were office buildings. The total costs of the archetype buildings were calculated as \$15,000,000, \$13,000,000, and \$43,000,000 US dollars for the three-story, six-story, and nine-story archetype buildings, respectively. The price of the retrofit using fluid viscous dampers was not considered, hence, the comparison of the expected annual losses is based only on the possible damage to the structural and non-structural elements. Figures 10 to 12 present the expected annual losses for the three archetype buildings as a function of the supplemental damping ratio and the velocity exponent. The results show a reduction in the expected annual losses for most of the viscous damper configurations. For the UD distribution of damping constants, it can be observed that increasing the targeted level of supplemental damping and reducing the velocity exponent causes the expected annual losses to increase, reaching the expected annual losses of the non-retrofitted case (control frame) for the six and nine-story archetype buildings. The addition of supplemental damping through fluid viscous dampers could



significantly improve the seismic performance of the archetype buildings by reducing the probability of collapse and reducing the inter-story drifts. However, due to the increased floor absolute accelerations in the three archetype buildings when large supplemental damping ratios and low velocity exponents are combined, the beneficial effects of the retrofit are negligible for acceleration-sensitive non-structural elements.

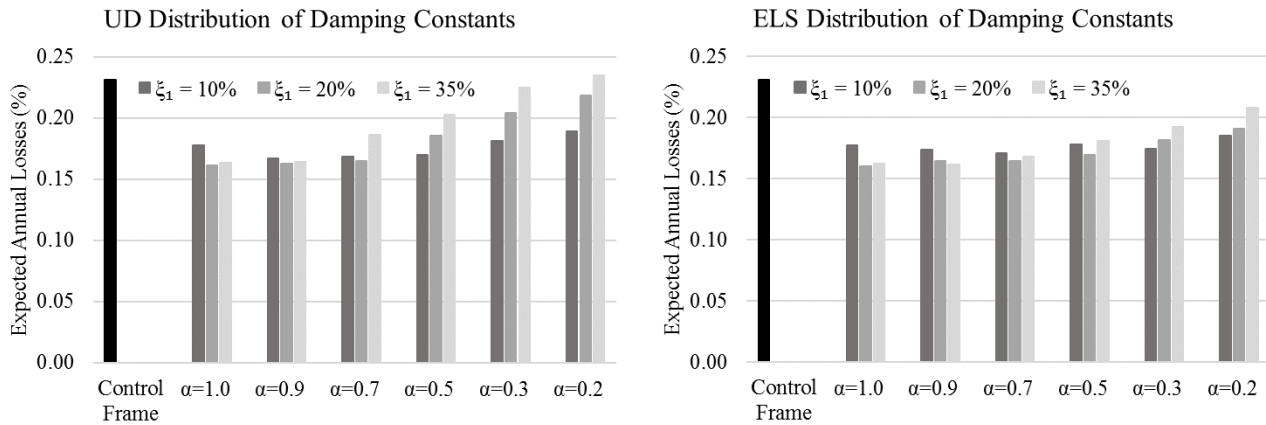


Fig. 10 – Expected annual losses of the archetype three-story building.

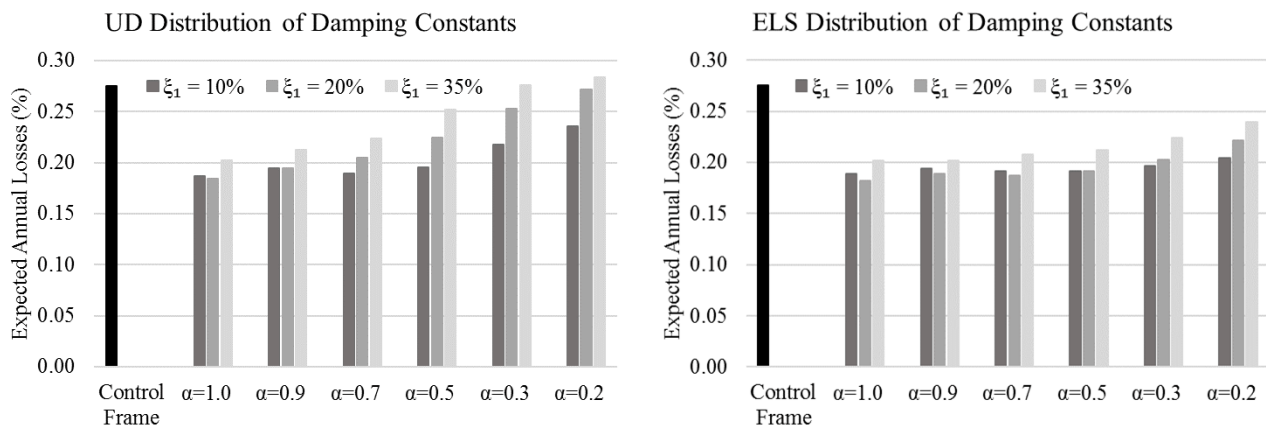


Fig. 11 - Expected annual losses of the archetype six-story building.

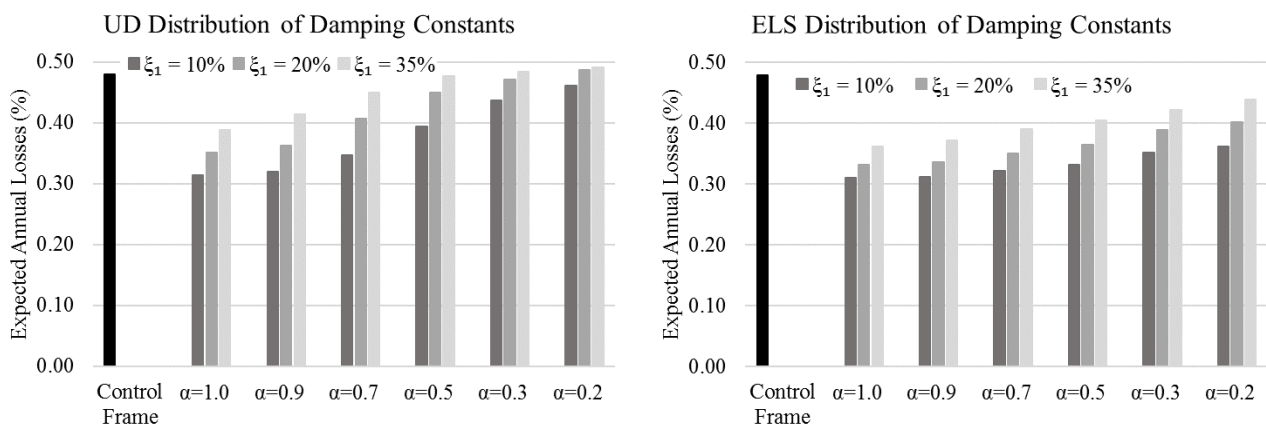


Fig. 12 - Expected annual losses of the archetype nine-story building.

## 5.5 Discussion

The implementation of viscous dampers has been largely studied in the past and showed excellent capacities at improving the seismic performance of structures. However, few studies have investigated the impact of the



different parameters that rule the design of viscous dampers on the acceleration demand on non-structural elements. The studies available in the literature are generally limited to the evaluation of peak floor accelerations without investigating the effects on absolute acceleration floor response spectra. This limitation could lead to non-conservative conclusions since the dynamic amplification caused by the interaction between the structure and the non-structural elements could be underestimated. In order to better estimate the contribution of acceleration-sensitive non-structural elements to the expected annual losses, recent studies [5] have suggested the implementation of spectral acceleration as a new engineering demand parameter. To facilitate more accurate estimations of expected losses due to acceleration-sensitive non-structural elements, and to reduce the significant computation efforts due to nonlinear time history analysis, several simplified methodologies have been developed to predict absolute acceleration floor response spectra [18]. However, to use the floor spectral accelerations as an engineering demand parameter it would be required to modify the non-structural fragility functions available in the literature, which are generally expressed as a function of the peak floor acceleration. Finally, the results of this study pointed out the importance of evaluating the impact of the implementation of any retrofitting technic, not only in terms of structural performance but also in terms of expected annual losses, which allow accounting for both structural and non-structural damage. In fact, the choice of the best retrofit technic, and its design assumptions could be governed by the non-structural losses if the benefits on the structural side are not reflected on the non-structural elements.

## 6. Conclusions

The incorporation of supplemental damping through fluid viscous dampers has demonstrated to be a feasible method to improve the seismic performance of a structure. However, there is little information on the effects of the different parameters involved in the design of viscous dampers on the acceleration demand on non-structural elements and consequently, the impact in the expected annual losses. In order to evaluate the earthquake expected annual losses of steel moment-resisting frames, three archetype frames of three, six, and nine stories were selected. The archetype buildings were equipped with diverse configurations of fluid viscous dampers including two distributions of damping constants, three targeted supplemental damping ratios, and six velocity exponents. Incremental dynamic analyses were carried out using the FEMA P-695 far-field ground motions set scaled to ten different intensities. Based on the obtained results, the collapse fragility functions, the median peak inter-story and residual drifts, the median peak floor absolute accelerations and median floor absolute acceleration spectra were calculated. The archetype buildings were supplied with non-structural elements typical of office use and the expected annual losses were calculated following the FEMA P-58 methodology for an intensity type assessment with nonlinear analysis. The results showed that the implementation of viscous dampers can reduce the probability of collapse and the relative displacements of the structure. However, some configurations of viscous dampers involving high targeted supplemental damping ratios and low velocities exponents can lead to an increase in the floor absolute accelerations in detriment of the seismic performance of acceleration-sensitive non-structural elements. The increment on the acceleration demand is notable on the expected annual losses in which, for the aforementioned dampers configurations, the expected annual losses can reach the losses of the non-retrofitted buildings. Finally, the results also highlight the limitations of using the peak floor acceleration as engineering demand parameter due to the amplification of the floor spectral accelerations in particular in the non-structural period ranges observed in the archetype buildings retrofitted with nonlinear viscous dampers with respect to that of the control frames. The peak floor spectral acceleration at the particular non-structural period is recommended as engineering demand parameter to better evaluate the seismic performance of acceleration-sensitive non-structural elements.

## 7. Acknowledgments

The work presented in this paper has been developed within the framework of the project “Dipartimenti di Eccellenza”, funded by the Italian Ministry of Education, University and Research at IUSS Pavia. The authors gratefully acknowledge also the Italian Department of Civil Protection (DPC) for their financial contributions to this study through the ReLUIIS 2019-2021 Project (Work Package 17 - Contributi Normativi Per Elementi



Non Strutturali). The Erasmus Mundus Program and the EUCENTRE Foundation are gratefully acknowledged for having provided financial support to the first author of this paper.

## 8. References

- [1] Christopoulos C., Filiatrault A. (2006): Principles of Passive Supplemental Damping and Seismic Isolation. *IUSS Press*, Pavia, Italy.
- [2] Chalarca B. (2017): Collapse Capacity of Steel Buildings Retrofitted with Linear and Nonlinear Viscous Dampers. *Master thesis*, University School for Advanced Studies IUSS Pavia, Pavia, Italy.
- [3] Kitayama S., Constantinou M.C. (2018): Seismic Performance of Buildings with Viscous Damping Systems Designed by the Procedures of ASCE/SEI 7-16. *ASCE Journal of Structural Engineering*, 144 (6).
- [4] Del Gobbo G. M., Blakeborough A., Williams M.S. (2018): Improving Total-Building Seismic Performance Using Linear Fluid Viscous Dampers. *Bulletin of Earthquake Engineering*, 16 (9), 4249-4272.
- [5] Chalarca B., Filiatrault A., Perrone D. (2019): Floor Acceleration Demand on Steel Moment-Resisting Frame Buildings Retrofitted with Linear and Nonlinear Viscous Dampers. *Proceedings of the Fourth International Workshop on Seismic Performance of Non-Structural Elements*. Pavia, Italy.
- [6] ATC (1994): Proceedings of the Invitational Workshop on Steel Seismic Issues. *Structural Engineers Association of California*, Applied Technology Council. Los Angeles, USA.
- [7] FEMA (2009): Quantification of Building Seismic Performance Factors FEMA P-695. *Federal Emergency Management*, Washington D.C., USA.
- [8] FEMA (2018): Seismic Performance Assessment of Buildings FEMA P-58. *Federal Emergency Management*, Washington D.C., USA.
- [9] FEMA (2005): Improvement of Nonlinear Static Seismic Analysis Procedures FEMA 440. *Federal Emergency Management*, Washington D.C., USA.
- [10] Tsai K. C., Popov E. P. (1988): Steel Beam-Column Joints in Seismic Moment Resisting Frames. *Report No. UCB/EERC-88/19*, Earthquake Engineering Research Center UC Berkeley, Berkeley, USA.
- [11] Hall J. F. (1995): Parameter Study of the Response of Moment-Resisting Steel Frame Buildings to Near-Source Ground Motions. *Technical Report SAC95-05: Parametric Analytical Investigation of Ground Motions and Structural Response*, Sacramento, USA.
- [12] McKenna F., Scott M.H., Fenves G.L. (2010): Nonlinear Finite Element Analysis Software Architecture Using Object Composition. *ASCE Journal Computing in Civil Engineering*, 24 (1), 95-107.
- [13] Zhang R. H., Soong T. T. (1992): Seismic Design of Viscoelastic Dampers for Structural Applications. *ASCE Journal of Structural Engineering*, 118 (5).
- [14] Lopez-García, D. (2001): A Simple Method for the Design of Optimal Damper Configurations in M dof Structures. *Earthquake Spectra*, 17 (3), 387-398.
- [15] Mohammadjavad H., Filiatrault A., Aref A. (2014): Simplified Seismic Collapse Capacity-Based Evaluation and Design of Frame Buildings with and without Supplemental Damping Systems. *Technical Report MCEER-14-0001*, Buffalo, USA.
- [16] ASCE (2017): Minimum Design Loads and Associated Criteria for Buildings and Other Structures ASCE/SEI 7-16. *American Society of Civil Engineers*, USA.
- [17] Baker J. W. (2011): Fitting Fragility Functions to Structural Analysis Data Using Maximum Likelihood Estimation. *Baker Research Group*, Stanford, USA.
- [18] Merino R. J., Perrone D., Filiatrault A. (2019): Consistent Floor Response Spectra for Performance-Based Seismic Design of Non-Structural Elements. *Earthquake Engineering and Structural Dynamics*, Accepted.